J Solid State Electrochem (2011) 15:683–688
DOI 10.1007/s10008-010-1136-3

ORIGINAL PAPER

# Electrochemical deposition and characterization of SnS thin films

**Medhat M. Kamel · Mervat Mohamed Ibrahim**

Received: 5 June 2010 / Revised: 28 June 2010 / Accepted: 29 June 2010 / Published online: 13 July 2010


**Abstract** Thin films of SnS were cathodically deposited onto stainless steel substrates from bath containing 0.025 M $SnSO_4$, 0.25 M KSCN and 0.25 M $Na_2SO_4$. The mechanism of electrochemical co-deposition of tin and sulphur was investigated by cyclic voltammetry. Analysis of the chronoamperometric current–time transients suggested that, in the potential range −560 to −590 mV vs saturated calomel electrode, the electrodeposition of SnS involved progressive nucleation model. However, at a potential −600 mV, the electrodeposition involved instantaneous nucleation model. The deposits have been characterized by scanning electron microscopy, X-ray diffraction and optical measurements. SnS films were found to be polycrystalline with an optical energy gap of 1.38 eV.

**Keywords** Electrochemical deposition · SnS · Thin films · Stainless steel substrate

## Introduction

The use of renewable energy to meet the energy demands has been steadily increasing over the years [1]. Solar energy seems to be the most attractive and promising alternative energy source for the future. It is environmentally benign, inexhaustible and available in amounts sufficient to cope with the needs of the present world requirements. For mass production of solar cells, we need a semiconductor deposition technique which can be easily scaled up at low cost. Deposition from aqueous or non-aqueous solutions meets this requirement. Electrochemical deposition (ECD) and chemical bath deposition (CBD) have been developed and studied extensively. ECD is very advantageous for solar cell fabrication because the film thickness is easily controlled by turning on/off the electrical current [2].

Tin sulphide is a layered semiconductor compound. It is a promising candidate in the field of photoelectrochemical solar energy conversion due to its highly stable nature [3]. It is basically the combination of Sn, an element from group IV, and S, the member of group VI. SnS usually exhibits *P*-type conduction and is reported to have a direct band gap of about 1.3 and an indirect band gap of about 1 eV [4–11]. SnS crystallizes in orthorhombic crystal structure with lattice parameters, $a$=4.329, $b$=11.193 and $c$=3.984 Å [12]. The lattice constants of this material are close to that of the II–VI compound, CdS. Therefore, the resulting heterojunction has a minimum lattice mismatch, thereby minimizing the interface state density. In addition, the constituent elements of this material are abundant in nature and non-toxic. These characteristics show that SnS is a promising material for solar cell application [7].

A number of deposition techniques, which include chemical deposition [10, 11, 13], evaporation technique [9, 12], chemical vapour transport [14] and electrochemical deposition [1–4, 15, 16] have been used for the preparation of SnS films.

In this work, we deposit SnS by the electrochemical deposition. ECD is the cheapest method available to deposit thin films and has been widely used for metal plating [4]. Only a few attempts of ECD of SnS have been reported. Mishra et al. [16] deposited SnS from organic solutions. More recently, Ghazali et al. [1], Subramanian et al. [3], Ichimura et al. [4] and Takeuchi et al. [2] deposited SnS from aqueous solutions. They used baths containing $SnSO_4/SnCl_2$ and $Na_2S_2O_3$. The role of thiosulphate is to generate colloids of elemental sulphur, which co-deposited with $Sn^{2+}$ and form SnS at the cathode.

M. M. Kamel (✉) · M. M. Ibrahim
Department of Chemistry, Faculty of Science,
Suez Canal University,
Ismailia 41522, Egypt
e-mail: madhet_kamel@yahoo.com

In this paper, we use the cathodic electrodeposition method to synthesis SnS thin films. This technique is more attractive as it offers the advantages of economy, convenience and several experimental parameters that can be controlled more precisely. In this study, we have employed thiocyanate ion ($SCN^-$) as the sulphur source [17]. The deposited films are characterized structurally and optically. In addition, a detailed study of the electrochemistry that involved in the deposition of SnS is presented.

## Experimental details

SnS thin films were obtained from bath of composition 0.025 M $SnSO_4$, 0.25 M KSCN and 0.25 M $Na_2SO_4$. All solutions were freshly prepared with distilled water and analytical grade chemicals. The pH was adjusted at 3 using sulphuric acid or sodium hydroxide and was measured via Fisher Scientific pH-metre.

The experimental setup for the electrochemical deposition process consisted of a rectangular Perspex cell containing 150 ml of electrolyte solution. The deposition was carried out from stagnant solutions. Experiments were carried out at 25±1 °C with the help of an air thermostat. The cathode was a 3×3-$cm^2$ stainless steel plate, and the anodes were stainless steel plate with total exposed area of 18 $cm^2$. The anodes were held in contact with the walls of the cell, and the cathode was positioned midway between them. The cathode was mechanically polished with progressively finer grades of emery paper, washed with distilled water and rinsed with ethanol. The plating time was 30 min, after which the cathode was withdrawn and the deposits were tested for its durability by subjecting it to a steady stream of distilled water.

The electrochemical measurements were conducted in a three-electrode cell, where the working electrode was a glassy carbon of area 1 $cm^2$. Saturated calomel was used as a reference electrode, and a platinum wire was employed as the counter electrode. These were connected to a potentiostat/galvanostat Model 263 A supplied by EG & G Princeton Applied Research. Voltammetric experiments were carried out at a scan rate of 50 mV $s^{-1}$, scanning initially towards negative potentials. Only one cycle was run in each voltammetric experiment. Chronoamperometric experiments were performed from an initial potential at which no process occurred to a potential at which reduction occurred.

The surface morphology of the deposited films was observed by a scanning electron microscope (JEOL Model JXA-840). The structure of the deposits was examined using Siemens D 500 X-ray diffraction at 35 kV and 15 mA. Optical properties were evaluated using JASCO V-570, UV/VIS/NIR double beam spectrophotometer.

## Results and discussion

### Cyclic voltammetry measurements

The electrochemical reactions that occur in the plating bath were studied by cyclic voltammetry. Figure 1 shows typical cyclic voltammograms that obtained in aqueous solution for $SnSO_4$, KSCN and mixture of $SnSO_4$ + KSCN on glassy carbon electrode. For $SnSO_4$ solution, the cyclic voltammogram (Fig. 1a) shows typical metal plating–anodic stripping behaviour. There is a sharp increase of cathodic current at −0.550 V due to a reduction of $Sn^{2+}$ ions to $Sn_{(s)}$.

$$Sn^{2+} + 2e \rightarrow Sn_{(s)} \left(E^{\theta} = -0.380 \text{ V vs. SCE}\right) \quad (1)$$

In the reverse scan, a well-defined anodic peak was observed at −0.362 V which could be assigned to the dissolution of the deposited $Sn_{(s)}$. The cyclic voltammogram of KSCN exhibits no peaks (Fig. 1b). The direct reduction of $SCN^-$ to generate $S^{2-}$ does not occur in this potential range [17].

$$SCN^- + 2e \rightarrow S^{2-} + CN^- \left(E^{\theta} = -1.096 \text{ V vs. SCE}\right) \quad (2)$$

When both $SnSO_4$ and KSCN exist in the solution (Fig. 1c), the cathodic current shifted negatively by 10 mV, as compared to that in Fig. 1a. Also, the anodic peak shifted by 10 mV towards more positive values. The presence of $SCN^-$ ions in the solution increases the overpotential for the reduction of $Sn^{2+}$ ions. This is mainly due to the complex formation ability of $SCN^-$ ions. Therefore, the observed shift of the $Sn^{2+}$ reduction current in Fig. 1c may attribute to the decreased activity of $Sn^{2+}$ ions in the presence of $SCN^-$ ions.

Thiocyanate forms stable complexes with various metal ions. These complexes are electrochemically reactive [17–19].

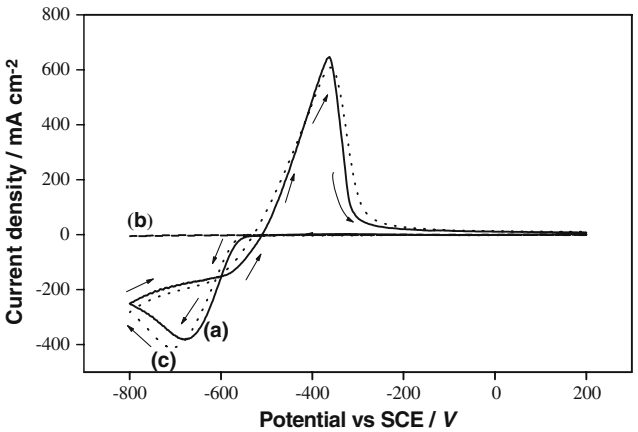


**Fig. 1** Cyclic voltammograms measured at a glassy carbon electrode in aqueous solutions of 0.025 M $SnSO_4$ (**a**), 0.25 M KSCN (**b**) and 0.025 M $SnSO_4$+0.25 M KSCN (**c**). Each solution contained 0.25 M $Na_2SO_4$. The measurements were performed at 25 °C and at a scan rate of 50 mV $s^{-1}$

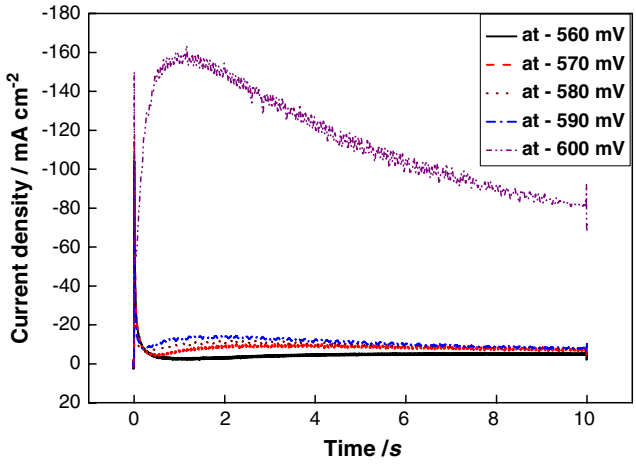


**Fig. 2** Chronoamperometric curves for deposition of SnS from solutions containing 0.025 M $SnSO_4$, 0.25 M KSCN and 0.25 M $Na_2SO_4$ after application of several cathodic potentials at 25 °C

For tin, Golub and Samoilenko [20] reported that the species of $Sn(NCS)^+$, $Sn(NCS)_2$ and $Sn(NCS)_3^-$ exist in aqueous solutions. It is probable that the formed complexes, e.g. $[Sn(NCS)_2]$, electroreduced at the cathode surface and form SnS. X-ray diffraction analysis confirmed the presence of SnS on the cathode surface. The same result was obtained by Yoshida et al. for CdS [17].

$$[Sn(NCS)_2] + 2e \rightarrow SnS + CN^- + SCN^- \left(E^\theta = -1.136\,\text{V vs. SCE}\right) \quad (3)$$

For Fig. 1, the distance of separation between the reduction and oxidation potentials for both Sn and SnS is large, indicating that the deposition process in each case is irreversible [1]. Also, the cathodic branch of Sn and SnS exhibits a nucleation/growth loop which indicates three-dimensional nucleation and subsequent grain growth. Therefore, both of Sn and SnS deposition processes were governed by nucleation and growth.

## Chronoamperometry measurements

Chronoamperometry experiments were carried out to investigate the SnS nucleation/growth process in more details. These experiments were carried out by stepping the potential of the working electrode from an initial value, where no

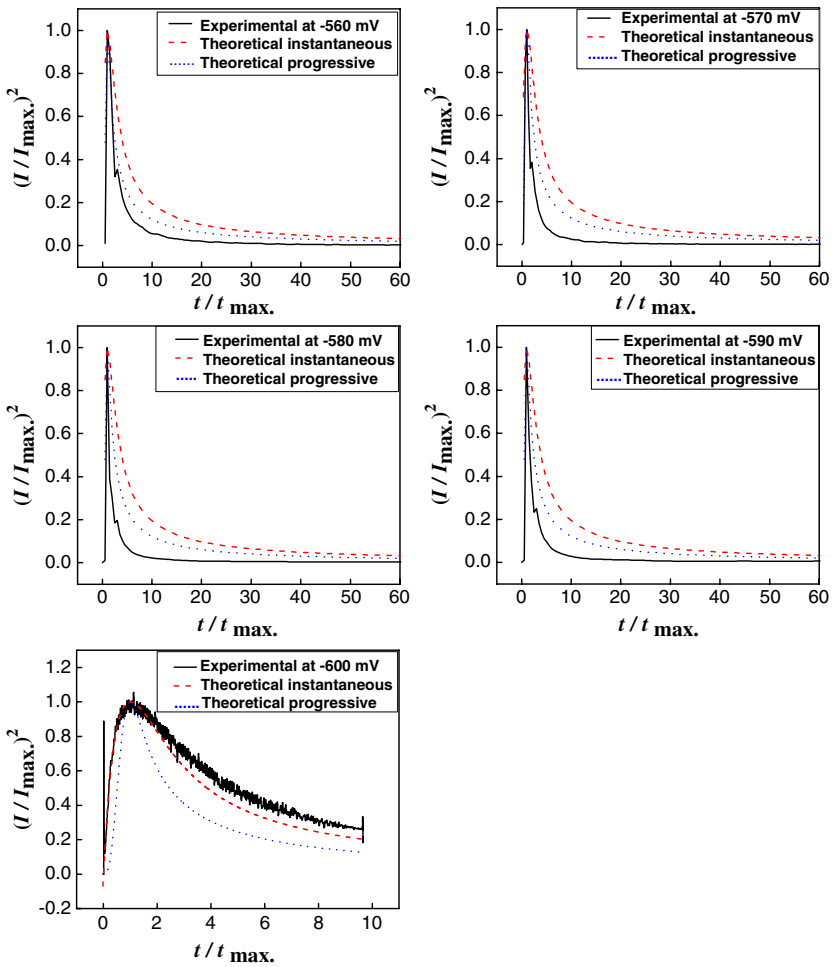


**Fig. 3** Comparison between experimental data for tin sulphide deposition on glassy carbon electrode and the theoretical non-dimensional plots for instantaneous and progressive nucleation models

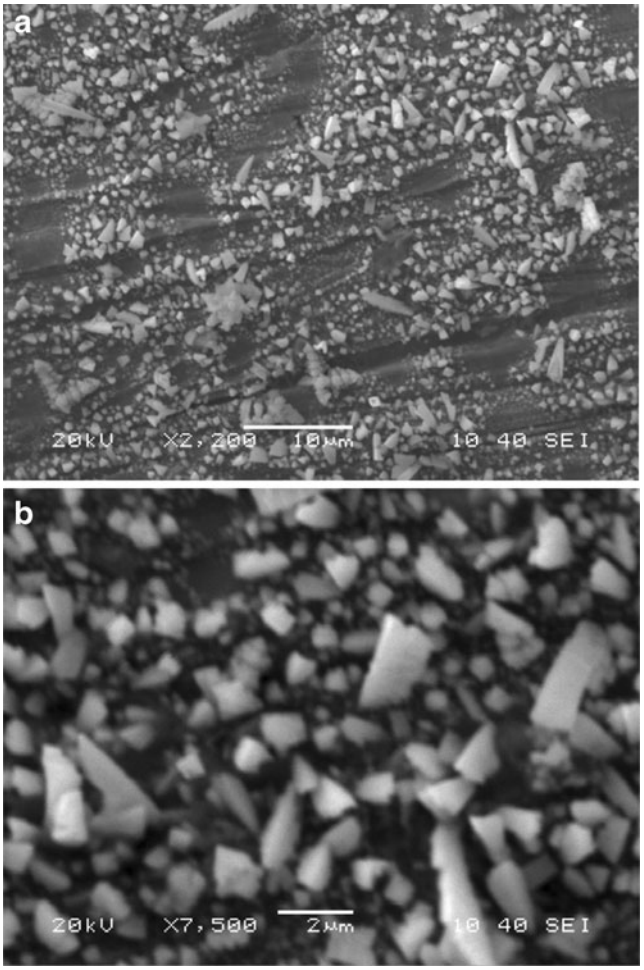


**Fig. 4** Scanning electron micrographs of SnS on stainless steel substrate obtained at 2.20 mA $cm^{-2}$. **a** ×2,200; **b** ×7,500

reduction would take place, to potentials sufficiently negative to initiate nucleation/growth process after short induction time [21]. Typical current–time transients from such experiments on glassy carbon are shown in Fig. 2. The transients exhibit the classical shape for a nucleation process. After the decay of a sharp electrode double-layer charging current, the current increases due to the nucleation and growth of SnS nuclei. Eventually, this raising current reaches maximum value, $i_{max}$. At this value, the discrete diffusion zones for each of the growing crystallites begin to overlap at time $t_{max}$. After $i_{max}$ has been reached, the current decays as the diffusion layer gets thicker. When the applied deposition potential becomes more negative, the nucleation density increases. This shortens the time required for the diffusion zones to overlap. As a result, the observed $i_{max}$ increases and $t_{max}$ decreases as the applied deposition potential becomes more negative.

By considering the overlap of the diffusion fields of randomly growing nuclei, Scharifker and Hills [22] deduced the following potentiostatic current–time relations for two different growth mechanisms.

$$(i/i_{max})^2 = (1.9542/(t/t_{max}))\{1 - \exp[-1.2564(t/t_{max})]\}^2$$

(Instantaneous nucleation) (4)

$$(i/i_{max})^2 = (1.2254/(t/t_{max}))\left\{1 - \exp\left[-2.3367(t/t_{max})^2\right]\right\}^2$$

(Progressive nucleation) (5)

To distinguish if the electrodeposition of SnS is involved with instantaneous or progressive nucleation/growth, the dimensionless experimental current–time transients are compared to the theoretical curves given by Eqs. 4 and 5. Examples of these plots together with theoretical curves derived from Scharifker equations for instantaneous and progressive nucleation are shown in Fig. 3. The data obtained at potentials −560, −570, −580 and −590 mV fit the progressive nucleation model, while those obtained at

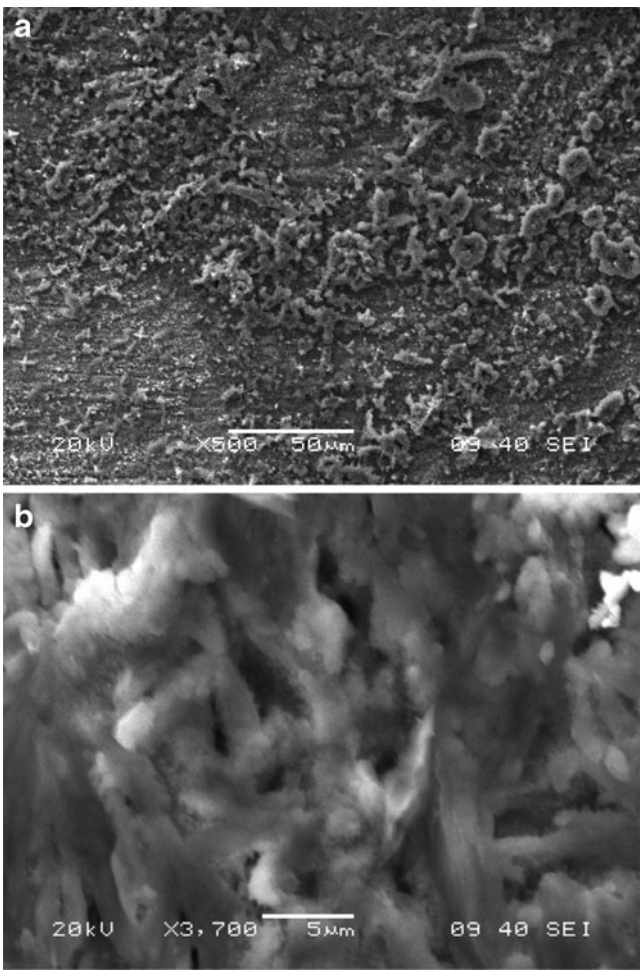


**Fig. 5** Scanning electron micrographs of SnS on stainless steel substrate obtained at 4.40 mA $cm^{-2}$. **a** ×500; **b** ×3,700

−600 mV is in good agreement with the instantaneous nucleation model. This transition from progressive to instantaneous nucleation indicates that the nucleation rate increases with increasing the applied deposition potential.

## Morphology and structure of the deposits

The durability of the thin film to the peel test manifested, as it did not show any tendency to peel off the substrate when subjected to a steady stream of distilled water. Microscopic examination reveals that the obtained deposits are uniform and compact with good coverage to the substrate basis. At low current density (2.20 mA $cm^{-2}$), polycrystalline deposits were observed. It has a distorted rock salt structure (Fig. 4). This result indicates low nucleation rate but high growth rate for low overpotentials. At high current density (4.40 mA $cm^{-2}$), the deposition is not uniform and the deposits composed of irregular grains. These grains are grouped together in random orientations and include some pores (Fig. 5). These features appear to be related to evolved hydrogen gas on the cathode surface.

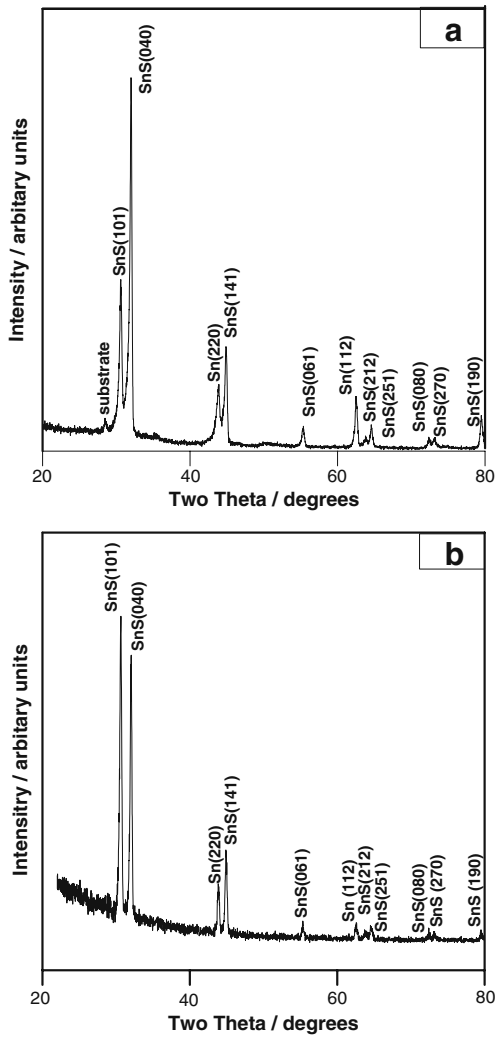


**Fig. 6** X-ray diffraction patterns of electrodeposited SnS films obtained at different current densities: **a** 2.20 and **b** 4.40 mA $cm^{-2}$

**Table 1** The calculated *d* spacing for SnS obtained at 4.40 mA $cm^{-2}$ in comparison to JCPDS card no. 14-620

| No. | Present study | | JCPDS card no. 14-620 | | |
|---|---|---|---|---|---|
| | *d* (Å) | $I/I_o$ | *d* (Å) | $I/I_o$ | *hkl* |
| 1 | 2.916 | 100 | 2.929 | 5 | (101) |
| 2 | 2.792 | 87.09 | 2.793 | 100 | (040) |
| 3 | 2.019 | 26.56 | 2.024 | 10 | (141) |
| 4 | 1.661 | 4.27 | 1.689 | 5 | (061) |
| 5 | 1.461 | 1.47 | 1.454 | 5 | (212) |
| 6 | 1.443 | 3.77 | 1.451 | 5 | (251) |
| 7 | 1.304 | 2.09 | 1.320 | 1 | (081) |
| 8 | 1.292 | 1.80 | 1.286 | 1 | (270) |
| 9 | 1.204 | 5 | 1.195 | 5 | (190) |

Figure 6 shows the typical X-ray diffraction patterns of the as-deposited SnS films obtained at different current densities. The dominant diffraction peaks of orthorhombic SnS are clearly observed. The deposited SnS is polycrystalline. Table 1 compares the *d* values calculated from X-ray diffraction pattern with the standard JCPDS values [23]. There is a fair agreement in *d* values. It should be noted that we cannot deny the presence of elemental Sn in the samples because the strongest Sn peak closely overlaps the SnS (101) and (040) peaks. Figure 6a depicts that the deposits obtained at 2.20 mA $cm^{-2}$ exhibit a preferred orientation in the (040) direction. Increasing the current density leads to an increase in the intensity of (101) plane (Fig. 6b).

## Optical properties of SnS films

The optical reflectance of the electrodeposited SnS films obtained at low current density (2.20 mA $cm^{-2}$) was

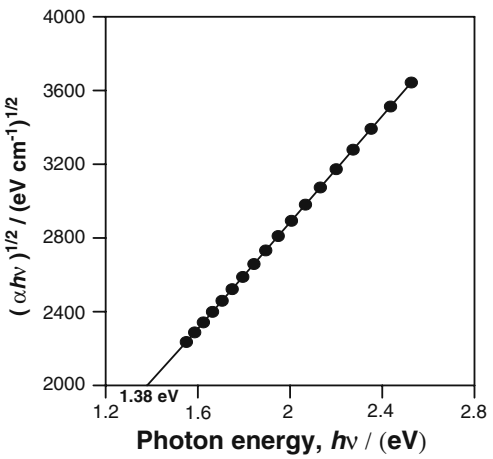


**Fig. 7** Plot of $(\alpha h\nu)^{1/2}$ vs. $h\nu$ for SnS film obtained at 2.20 mA $cm^{-2}$

measured in the wavelength range of 200–1,200 nm at room temperature. The films showed a high absorption coefficient, $\alpha$. Its value is higher than $10^4$ $cm^{-1}$, so that even thin layers can absorb most of the incident radiation. The energy band gap of the films was determined from the plot of $(\alpha h\nu)^{1/2}$ vs $h\nu$ and is shown in Fig. 7. The plot was linear, indicating indirect optical transition. The evaluated energy band gap was 1.38 eV. This value is in good agreement with values reported in the literatures [4].

## Conclusion

SnS thin films were cathodically deposited onto stainless steel substrates by electrodeposition technique. The deposition was carried out from solution containing 0.025 M $SnSO_4$, 0.25 M KSCN and 0.25 M $Na_2SO_4$. The deposition process was studied by cyclic voltammetry and chronoamperometric techniques. The deposited SnS was polycrystalline and had orthorhombic structure. The films were highly absorbing and the evaluated optical energy band gap was 1.38 eV.

## References

1. Ghazali A, Zainal Z, Hussein MZ, Kassim (1998) Sol Energy Mater Sol Cells 55:237
2. Takeuchi K, Ichimura M, Arai E, Amazaki YY (2003) Sol Energy Mater Sol Cells 75:427
3. Subramanian B, Sanjeeviraja C, Jayachandran M (2001) Mater Chem Phys 71:40
4. Ichimura M, Takeuchi K, Ono Y, Arai E (2000) Thin Solid Films 361:362
5. Reddy NK, Reddy KT (1998) Thin Solid Films 325:4
6. Reddy KT, Reddy P, Miles RW, Datta PK (2001) Opt Mater 17:295
7. Reddy KT, Reddy P, Datta PK, Miles RW (2002) Thin Solid Films 403–404:116
8. Reddy KT, Reddy P (2002) Mater Lett 56:108
9. El-Nahass MM, Zeyada HM, Aziz MS, El-Ghamaz NA (2002) Opt Mater 20:159
10. Ray SC, Karanjai MK, DasGupta D (1999) Thin Solid Films 350:72
11. Ristov M, Sinadinovski G, Mitreski M, Ristova M (2001) Sol Energy Mater Sol Cells 69:17
12. Abou Shama A, Zeyada HM (2003) Opt Mater 24:555
13. Nair PK, Nair MTS, Garcia VM, Arenas OL, Pena Y, Castillo A, Ayalo IT, Gomezadaza O, Sanchez A, Campos J, Suarez HHR, Rincon ME (1998) Sol Energy Mater Sol Cells 52:313
14. Shibata T, Muranushi Y, Miura T, Kishi T (1991) J Mater Sci 26:5107
15. Zainal Z, Hussein MZ, Ghazali A (1996) Sol Energy Mater Sol Cells 40:347
16. Mishra K, Rajeshwar K, Wiess A (1989) J Electrochem Soc 136:1915
17. Yoshida T, Yamaguchi K, Kazitani T, Suigura T, Minoura H (1999) J Electroanal Chem 473:209
18. Winkler K, Krogulec T (1990) J Electroanal Chem 281:171
19. Hrynaszkiewicz TJ, Kozlowski J, Cieszynska E, Krogulec T (1994) J Electroanal Chem 367:213
20. Golub AM, Samoilenko VM (1963) Ukrain Khim Zhur 29:789
21. Lin YF, Sun IW (1999) Electrochim Acta 449:2771
22. Scharifker B, Hills G (1983) Electrochim Acta 28:879
23. JCPDS (1991) Powder Diffraction File 14-620